JACS
JOURNAL OF THE AMERICAN CHEMICAL SOCIETY

Communication

pubs.acs.org/JACS

Selective Cell Death by Photochemically Induced pH Imbalance in Cancer Cells

Xiling Yue,[†] Ciceron O. Yanez,[†] Sheng Yao,[†] and Kevin D. Belfield*[,†,‡]

[†]Department of Chemistry and [‡]CREOL, The College of Optics and Photonics, University of Central Florida, P.O. Box 162366, Orlando, Florida 32816, United States

Supporting Information

ABSTRACT: Singlet oxygen sensitized photodynamic therapy (PDT) relies on the concentration of oxygen in the tissue to be treated. Most cancer lesions, however, have poor vasculature and, as a result, are hypoxic, significantly hindering PDT efficacies. An oxygen-independent PDT method may circumvent this limitation. To address this, we prepared sulfonium salts that produced a pH drop within HCT 116 cells via the generation of a photoacid within the cytosol. This process was driven by one- or two-photon absorption (1PA or 2PA) of the endocytosed photoacid generators (PAGs). One of these PAGs, which had a significantly lower dark cytotoxicity and was more efficient in generating a photoacid, effectively induced necrotic cell death in the HCT 116 cells. The data suggest that PAGs may be an attractive alternative PDT modality to selectively induce cell death in oxygen-deprived tissue such as tumors.

The success of photodynamic therapy (PDT) requires the careful balance of three conditions that must be present in the targeted cells at the time of therapy: (1) oxygen saturation of the tissue, (2) sufficient PS concentration throughout the lesion, and (3) sufficient intensity of the sensitizing light. Even in a single gland such as the prostate, all three of these agents are present in quite heterogeneous concentrations and doses.[1] This has significantly complicated and compromised the reproducibility of singlet oxygen photosensitized PDT ($^1O_2$-PS PDT).

For over 100 years photodynamic oncotherapy has sought to produce singlet oxygen in an oxygen-depleted environment. Vasculature in healthy tissue is very well structured; the inner walls of healthy vessels are conformed by well differentiated endothelial cells. In contrast, tumor vessels have very poor morphology and are conformed by immature cells in a mesh-like architecture that confers a leaky property to the vessel. The leaky character of these vessels generates a hypoxic and acidic microenvironment that induces the production of positive or negative regulators of angiogenesis.[2]

This hypoxic environment within a tumor often leads to poor outcomes in $^1O_2$-PS PDT because frequently there is a limited amount of oxygen to excite. The minimal concentrations of oxygen are quickly depleted upon $^1O_2$-PS PDT, making it extremely easy to saturate the irradiation dose upon treatment. Furthermore, these extreme hypoxic events are often followed by ischemia, which not only further compromises the flow of oxygen to the tumor but also hinders the delivery of complementary chemotherapeutic agents that are delivered via the bloodstream.[1b]

Herein, an oxygen-independent means of inducing cell death via PDT is shown. Instead of inducing singlet oxygen by photosensitization, a pH imbalance was induced within the cytosol of the cells that were targeted by a photoacid generator (PAG), affording oxygen-independent PDT (OI-PDT, Figure 1).

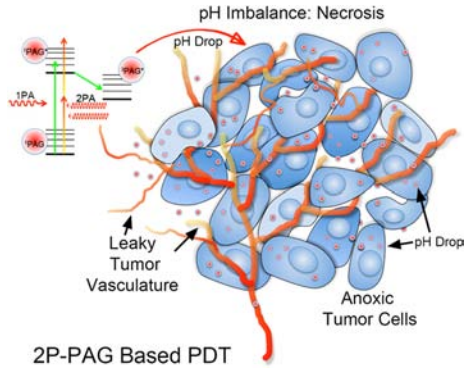

Figure 1. Two-photon (2P) PAG based PDT in anoxic tumor cells. 2P-PAG based PDT induces cell death by means of a pH imbalance.

The therapeutic agents were encapsulated sulfonium salts, molecules that have traditionally been used as photoacid generators (PAGs) in lithography and cationic polymerization. The PAGs were incubated in human colorectal carcinoma (HCT-116) cells and, once in the cytosol, were excited to generate a photoacid that caused a pH imbalance within the cell. These PAGs were tailor-made to absorb at longer wavelengths.

Most commercially available PAGs have an absorption λ_{max} in the UV or deep-UV because their applications in lithography require them to absorb at the shortest possible wavelengths. Recently, a series of more conjugated, longer-wavelength-absorbing PAGs were synthesized in our lab that were designed to be efficient two-photon absorbing molecules.[3] The generation of a photoacid was induced by one- and two-photon absorption (1PA or 2PA) of PAGs **1**−**3** (Figures 1 and S1). To our knowledge, this is the first example of the use of

Received: December 14, 2012
Published: January 30, 2013

   dx.doi.org/10.1021/ja3122312 | J. Am. Chem. Soc. 2013, 135, 2112−2115

PAGs to cause cell death by generating a pH imbalance in the cell.

The emergence of nonlinear (2PA) techniques has taken advantage of the quadratic dependence that 2PA has on the intensity of the incident light.[4] This advantage can also be exploited in PDT applications and require that the molecules employed for therapy be efficient two-photon absorbers; i.e., the molecules need to have high 2PA cross sections. The possibility of using such agents, along with deeper penetrating longer wavelength light used in two-photon excitation, in cancer lesions that are buried under sensitive, healthy tissue (i.e., gliomas) makes these 2PA PAGs especially important. Undoubtedly, the simplicity associated with generating photoacid by 1PA is also an advantage. One-photon photoacid generation is a more efficient process, where the excitation source needed is cheaper and easier to use. In exchange for tissue penetration, a larger amount of targeted surface mass within tissue can be covered at a faster rate.

Two-photon photoacid generation is a lower probability process, because it is energy dependent and relies on more elaborate pulsed lasers as energy sources. However, it has a tremendous tissue penetration advantage, and the process is confined to a smaller volume. Ideally, both methods can be used simultaneously to maximize the possibility of success of the OI-PDT process.

Originally, the synthesis of triarylsulfonium salts was reported by Crivello and Lam, where the thermolysis of a diphenyliodonium in the presence of a diphenylsulfide formed the desired sulfonium salt.[5] Recently, a more efficient, microwave-assisted, synthetic strategy of triarylsulfonium salt PAGs was reported.[3] PAGs **1**−**3** were designed to exhibit high 2PA cross sections. Fluorene was chosen as the core structure because of its high thermal and photochemical stability.[6] Quite advantageously, fluorene lends itself to ready substitution in its 2-, 7-, and 9-positions. In PAGs **1** and **2**, stilbenyl motifs were introduced (2- and 7-positions) to extend the π-conjugation. Ultimately, two acceptor groups (triarylsulfonium and nitro) were introduced for net structures of A-π-π-A (PAG **1**) and A-π-π-π-A (PAG **2**).

To enhance the photoacid quantum yield per molecule, the first approach was to incorporate two sulfonium salt motifs onto the fluorenyl scaffold, such as in PAG **2** (Figure 2). However, this molecule exhibited a very low photoacid quantum yield (0.03). The high fluorescence quantum yield of this PAG (0.80) indicated the molecule was undergoing radiative decay (fluorescence) before it had a chance to form a photoacid.

The direct photolysis of triarylsulfonium salts has been reported to occur primarily from the first excited singlet state. However, sensitization studies have shown that triplet triarylsulfonium salts are also labile.[7] Consequently, to increase the probability of spin orbit coupling to induce intersystem crossing, a nitro group was incorporated into the fluorene backbone. As a result, the fluorescence quantum yield of the sulfonium salt PAG **1** was significantly decreased (Table 1), thereby reducing the radiative decay pathway.

Nitro-containing PAG **1** exhibited an increased photoacid quantum yield (Table 1). The 2PA cross sections, however, were found to be up to 5 times higher for PAG **2** than for PAG **1** (Table 1). This disparity in 2PA cross section values vs photoacid quantum yield values makes it difficult to rank these PAGs by their overall efficiencies. Using only one of these two photophysical properties would be incomplete and could lead to erroneous interpretations.

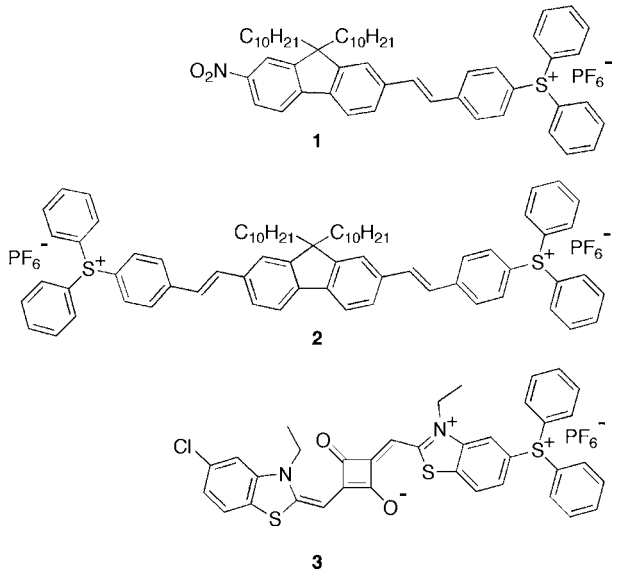

Figure 2. Sulfonium salt 2PA PAGs structures.

Table 1. Photophysical Properties of PAGs

PAG	Φ_F[a]	Φ_{H+}[b]	δ_{710} (GM)	$\Phi_{H+}\delta$ (GM)
1	0.10 ± 0.01	0.40 ± 0.04	240 ± 24	96 ± 10
2	0.80 ± 0.06	0.03 ± 0.003	1275 ± 130	38 ± 4
3	0.27 ± 0.02	0.01 ± 0.005	–	–

[a]Fluorescence quantum yields, Φ_F, with diphenylanthracene in cyclohexane as the standard. [b]Φ_{H+}, photoacid quantum yields at 350 nm with RhB+ as the indicator. δ, 2PA cross sections at 710 nm; $\Phi_{H+}.\delta$, two-photon action cross-section of photoacid generation at 710 nm.

A more useful value to compare the PAGs is the 2PA action cross section of photoacid generation, given by the product of photoacid generation quantum yield and the 2PA cross section at a specific wavelength. On the basis of the 2PA action cross section, the overall efficiency of PAG **1** was higher than that of PAG **2**. In a constant effort to improve the properties of these molecules, other PAGs are currently being synthesized in the lab that absorb at longer wavelengths and possess higher 2PA cross sections. An example of this type of molecule is PAG **3**. The squaraine core has the advantage of having a linear absorption λ_{max} in the NIR and has been associated with high 2PA. A comparable figure of merit for one of the most widely used PDT agents photofrin (singlet oxygen quantum yield × 2PA cross section) illustrates the efficiency of the PAGs. In the literature, the photofrin oxygen quantum yield is ca. 0.2, and its 2PA cross sections range from 10 to 15 GM.[8] Based on these values, the action cross section for photofrin would be at most 3 GM; significantly, the action cross section for PAG **1** is 30 times larger (96 GM, Table 1).

Pluronic F-127 has been widely used in drug delivery applications to enhance the solubility of hydrophobic substances such as anticancer drugs.[9] Pluronic micelles are known to be uptaken by MDCK cells by means of clathrin-mediated endocytosis when present above the critical micelle concentration.[10] The hydrophobic character PAGs **1**−**3** facilitated their encapsulation in Pluronic F-127.[11] Steady state, linear absorption of solutions of Pluronic F-127-

dx.doi.org/10.1021/ja3122312 | J. Am. Chem. Soc. 2013, 135, 2112−2115

encapsulated PAGs (PL PAGs) in PBS was measured (Figure 2). The PL PAGs were tracked through the vesicle maturation process of endocytosis. After the micelles undergo endocytosis, they can reach full endosomal maturation, reaching the lysosomes, follow exocytosis before attaining the endolysosomal stage, or buildup in other regions such as the mitochondria. We mainly observed the accumulation of the PL PAGs in the endosomes-lysosomes (even after 24 h of incubation, Figure S2) in HCT 116 cells.

An ideal PAG for phototherapy would exhibit low cytotoxicity when unexposed and induce a high percentage of cell death upon irradiation. To assess the intrinsic toxicity of the PAGs, cell viability assays were carried out in the dark (dark viability) to avoid the production of a photoacid. The cells were incubated with 1, 5, 10, and 15 μM solutions of PL PAG **1**−**3** for 24 h at 37 °C. The results indicated PL PAG **1** had the lowest dark cytotoxicity throughout this concentration range, followed by PL PAG **3** and PL PAG **2**, respectively (Figure S3).

Based on these results, exposure experiments were performed at 1, 5, and 10 μM for all PL PAGs. The most appreciable changes in viability (from dark viability to postexposure viability) were observed at 10 μM (Figure 3).

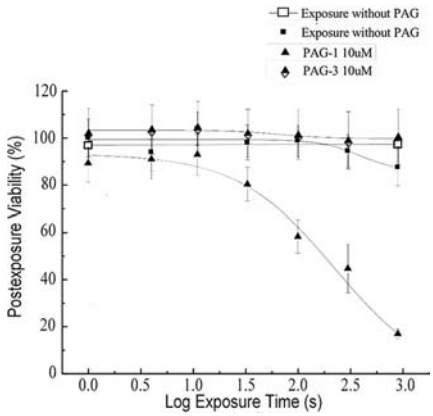

Figure 3. Postexposure viability of HCT 116 cells incubated with PL PAGs **1** and **3**. PL PAG **1** exhibited the lowest intrinsic (dark) cytotoxicity and highest postexposure cytotoxicity.

PL PAG **1** showed the best results, promoting a drop from 90% viability to 20% viability after 900 s of exposure. Even at these relatively high concentrations, PL PAGs **2** and **3** failed to induce a significant drop in cell viability. This is consistent with their photoacid quantum yields (Table 1), which are much less efficient in producing a photoacid than PAG **1**; i.e., the induction of cell death was proportional to the amount of acid generated.

A correlation of irradiation and decrease in lysosomal pH was demonstrated by the aid of LysoSensor Green. LysoSensor Green has been reported to monitor acidic pH within cells.[12] This dye is known to increase its fluorescence quantum yields when in acidic compartments. An increase in fluorescence intensities as a function of exposure dose was, indeed, observed in cells that were coincubated with PL PAG **1** (10 μM) and LysoSensor Green (Figure S4). This indicates a drop in intralysosomal pH (of the already acidic compartments) followed by irradiation in HCT 116 cells previously incubated with PL PAG **1** (10 μM). The drop in fluorescence intensities as a function of irradiation dose in control cells can be attributed to the photobleaching of the pH indicator that had been acidified by the acidic character of the lysosomes. It was estimated that a 10 μM concentration of PAG **1** would, at least, generate 2.1072×10^{-6} M at the irradiation doses used for 80% cell death. This would lead to a drop of intralysosomal pH to ≤4.5 (Figure S6).

Cell death induced by two-photon photoacid generation was demonstrated in an experiment where HCT 116 cells were incubated with PL PAG **1** for 24 h, followed by two-photon irradiation (710 nm, 2.0 mW/cm^2). After irradiation, the cells were incubated with propidium iodide to assess the proportion of cells that underwent necrotic cell death (Figure 4). A control

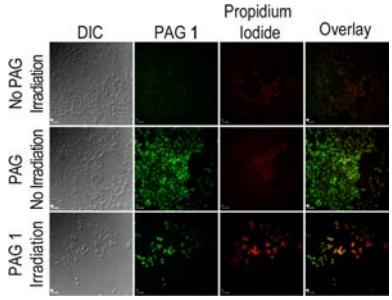

Figure 4. HCT 116 human colorectal carcinoma cells incubated for 24 h with PL PAG **1** (10 μM) and irradiated at 710 nm (70 fs pulses, 80 MHz repetition rate, 2.0 mW/cm^2). Generation of photoacid induced by 2PA promoted necrosis in HCT 116. Residual PAG **1** fluorescence illustrated PAG uptake. Cells were unaffected by nonirradiated PAG or irradiation w/o PAG. Scale bar 50 μm.

sample to determine the effect of the irradiation conditions on the cell was performed by irradiating cells that had not been incubated with the PAG. The micrographs showed excellent cell morphology (DIC) and high viability (low fluorescence intensity of the PI channel) of the cells for up to 24 h following irradiation. A second control, in which cells were incubated with PL PAG **1** but were not irradiated, showed adequate cell uptake and no detectable cell death via the necrotic pathway. Irradiated cells showed significant cell swelling and loss of membrane potential as indicated by the uptake of propidium iodide. All the cells in the exposed area appeared to die by necrosis, which is expected when such a grave physiological imbalance takes place.

Time-lapsed micrographs in Figure S5 show this progressive change in cell morphology following the generation of photoacid. Loss of cell adhesion (green arrows) is followed by a "blebbing"-like activity (yellow arrows). The integrity of the nuclei in these cells is a sign that chromatin condensation is not occurring and hence the process is not apoptotic. What followed was significant cell swelling that is characteristic of necrosis (blue arrows). Despite the low fluorescence quantum yield, PAG **1** was fluorescent enough to allow visualization of its uptake and colocalization with LysoTracker Red (Figures S2 and S5). The high degree of colocalization suggests that it was mainly localized in the lysosomes.

The use of photoacid generators to induce cell death by creating a grave pH imbalance in cells has not been reported prior to this work. We demonstrated that sulfonium-based PAGs can be used to selectively induce cell death upon photoexcitation. This opens the possibility of photochemically inducing cell death in an oxygen-independent manner. More specifically, PL PAGs have induced necrotic cell death via generation of photoacid in the lysosomes in HCT 116 cells.

dx.doi.org/10.1021/ja3122312 | J. Am. Chem. Soc. 2013, 135, 2112−2115

Acid was generated by both 1PA and 2PA, which means cell death can be induced by either method. In order to achieve deep tissue penetration, near-IR two-photon excitation is particularly attractive. Thus, the ability to induce two-photon photoacid generation of PAGs in cells is significant. PL PAG **1** is a versatile compound that can be used to exploit the advantages of one- or two-photon photoacid-based PDT. These results lay the foundations for the use of PAGs in OI-PDT.

■ ASSOCIATED CONTENT

Ⓢ Supporting Information

Supplementary images, detailed experimental procedures, and complete molecule characterization for all new compounds. This material is available free of charge via the Internet at http://pubs.acs.org.

■ AUTHOR INFORMATION

Corresponding Author

belfield@ucf.edu

Funding

No competing financial interests have been declared.

Notes

The authors declare no competing financial interest.

■ ACKNOWLEDGMENTS

We acknowledge the National Institute of Biomedical Imaging and Bioengineering of the National Institutes of Health (R15 EB008858-1) and the National Science Foundation (CHE-0832622 and ECCS-0925712) for support of this work.

■ REFERENCES

(1) (a) Zhu, T. C.; Finlay, J. C.; Hahn, S. M. *J. Photochem. Photobiol. B: Biol.* **2005**, *79*, 231. (b) Moore, R. B.; Chapman, J. D.; Mercer, J. R.; Mannan, R. H.; Wiebe, L. I.; McEwan, A. J.; McPhee, M. S. *J. Nucl. Med.* **1993**, *34*, 405.

(2) Brown, J. M.; William, W. R. *Nat. Rev. Cancer* **2004**, *4*, 437.

(3) Yanez, C. O.; Andrade, C. D.; Belfield, K. D. *Chem. Commun.* **2009**, 827.

(4) (a) Maruo, S.; Nakamura, O.; Kawata, S. *Opt. Lett.* **1997**, *22*, 132. (b) Parthenopoulos, D. A.; Rentzepis, P. M. *Science* **1989**, *245*, 843. (c) Strickler, J. H.; Webb, W. W. *Opt. Lett.* **1991**, *16*, 1780.

(5) (a) Crivello, J. V.; Lam, J. H. W. *J. Org. Chem.* **1978**, *43*, 3055. (b) Crivello, J. V.; Lam, J. H. W. *J. Polym. Sci., Part A* **1978**, *16*, 2441. (c) Crivello, J. V.; Lam, J. H. W. *J. Polym. Sci., Part B* **1978**, *16*, 563.

(6) Belfield, K. D.; Bondar, M. V.; Przhonska, O. V.; Schafer, K. J. *J. Photochem. Photobiol. A: Chem.* **2004**, *162*, 489.

(7) Dektar, J. L.; Hacker, N. P. *J. Am. Chem. Soc.* **1990**, *112*, 6004.

(8) (a) DeRosa, M. C.; Crutchley, R. J. *Coord. Chem. Rev.* **2002**, *233*, 351. (b) Mathai, S.; Bird, D. K.; Stylli, S. S.; Smith, T. A.; Ghiggino, K. P. *Photochem. Photobiol. Sci.* **2007**, *6*, 1019.

(9) (a) Escobar-Chavez, J. J.; Lopez-Cervantes, M.; Naik, A.; Kalia, Y. N.; Quintanar-Guerrero, D.; Ganem-Quintanar, A. *J. Pharm. Pharmaceut. Sci.* **2006**, *9*, 339. (b) Batrakova, E. V.; Kabanov, A. V. *J. Controlled Release* **2008**, *130*, 98.

(10) (a) Sahay, G.; Batrakova, E. V.; Kabanov, A. V. *Bioconjugate Chem.* **2008**, *19*, 2023. (b) Batrakova, E. V.; Li, S.; Vinogradov, S. V.; Alakhov, V. Y.; Miller, D. W.; Kabanov, A. V. *J. Pharmacol. Exp. Ther.* **2001**, *299*, 483. (c) Kabanov, A. V.; Levashov, A. V.; Alakhov, V. Y. *Protein Eng.* **1989**, *3*, 39.

(11) (a) Andrade, C. D.; Yanez, C. O.; Qaddoura, M. A.; Wang, X. H.; Arnett, C. L.; Coombs, S. A.; Yu, J.; Bassiouni, R.; Bondar, M. V.; Belfield, K. D. *J. Fluoresc.* **2011**, *21*, 1223. (b) Andrade, C. D.; Yanez, C. O.; Rodriguez, L.; Belfield, K. D. *J. Org. Chem.* **2010**, *75*, 3975. (c) Wang, X. H.; Nguyen, D. M.; Yanez, C. O.; Rodriguez, L.; Ahn, H. Y.; Bonder, M. V.; Belfield, K. D. *J. Am. Chem. Soc.* **2010**, *132*, 12237.

(12) Tian, Y.; Su, F.; Weber, W.; Nandakumar, V.; Shumway, B. R.; Jin, Y.; Zhou, X.; Holl, M. R.; Johnson, R. H.; Meldrum, D. R. *Biomaterials* **2010**, *31*, 7411.